ACS Medicinal Chemistry Letters

pubs.acs.org/acsmedchemlett Letter

Bromocriptine as a Novel Pharmacological Chaperone for Mucopolysaccharidosis IV A

Sergio Olarte-Avellaneda, Jacobo Cepeda Del Castillo, Andrés Felipe Rojas-Rodriguez, Oscar Sánchez, Alexander Rodríguez-López, Diego A. Suárez García, Luz Mary Salazar Pulido, and Carlos J. Alméciga-Díaz*

Cite This: ACS Med. Chem. Lett. 2020, 11, 1377−1385 Read Online

ACCESS | Metrics & More | Article Recommendations | Supporting Information

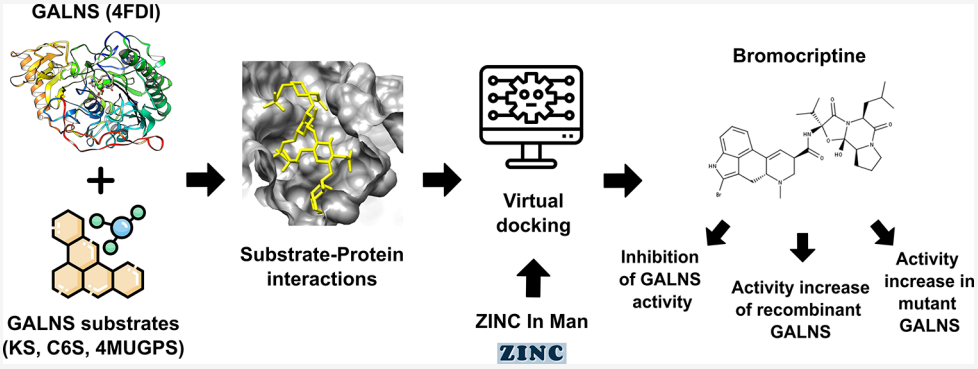

ABSTRACT: Mucopolysaccharidosis IVA (MPS IVA) is a lysosomal storage disease caused by mutations in the gene encoding for the enzyme *N*-acetylgalactosamine-6-sulfate sulfatase (GALNS), leading to lysosomal accumulation of keratan sulfate (KS) and chondroitin-6-sulfate. In this study, we identified and characterized bromocriptine (BC) as a novel PC for MPS IVA. BC was identified through virtual screening and predicted to be docked within the active cavity of GALNS in a similar conformation to that observed for KS. BC interacted with similar residues to those predicted for natural GALNS substrates. *In vitro* inhibitory assay showed that BC at 50 μM reduced GALNS activity up to 30%. However, the activity of hrGALNS produced in HEK293 cells was increased up to 1.48-fold. BC increased GALNS activity and reduced lysosomal mass in MPS IVA fibroblasts in a mutation-dependent manner. Overall, these results show the potential of BC as a novel PC for MPS IVA and contribute to the consolidation of PCs as a potential therapy for this disease.

KEYWORDS: *Bromocriptine, MPS IVA, pharmacological chaperone, virtual screening*

Mucopolysaccharidosis IVA (MPS IVA, Morquio A, OMIM 253000) is a lysosomal storage disease (LSD) caused by mutations in the gene encoding for the enzyme *N*-

Table 1. Summary of Interactions Predicted between Substrates and GALNS Crystal Structure[a]

Substrate	Hydrogen bonds	Hydrophobicinteractions
KS	FGly79, Tyr108 Gln111, Arg175 His236, Lys310Ser521	Leu78, Pro110, Glu112, His142, Phe167, Ile294, Cys489, Trp520, His522.
C6S	Asn106, Tyr108 His236, Lys310 Gln311, Ser521	Leu78, FGly79, His142, Ile294, Trp520.
G6S	Asn106, Lys310 Ser521	Leu78, Tyr108, His236, Gln311.
4MUGPS	Lys140, His236 Lys310	FGly 79, Asn106, Tyr108, His142, Ile294, Gln311, Ile416, Phe418, Trp520, Ser521.

[a]Interactions were predicted by using LigPlot+ v.2.2.

Table 2. Affinity Energies for Substrates against GALNS Crystal Structure with FGly79 or Cys79

	Affinity energy (kcal mol^{-1})	
Substrate	GALNS−Cys79	GALNS−FGly79
KS	−7.7	−8.3
C6S	−6.3	−6.7
G6S	−5.2	−5.7
4MUGPS	−5.4	−5.7

Received: January 29, 2020
Accepted: June 24, 2020
Published: June 24, 2020

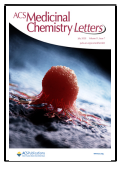

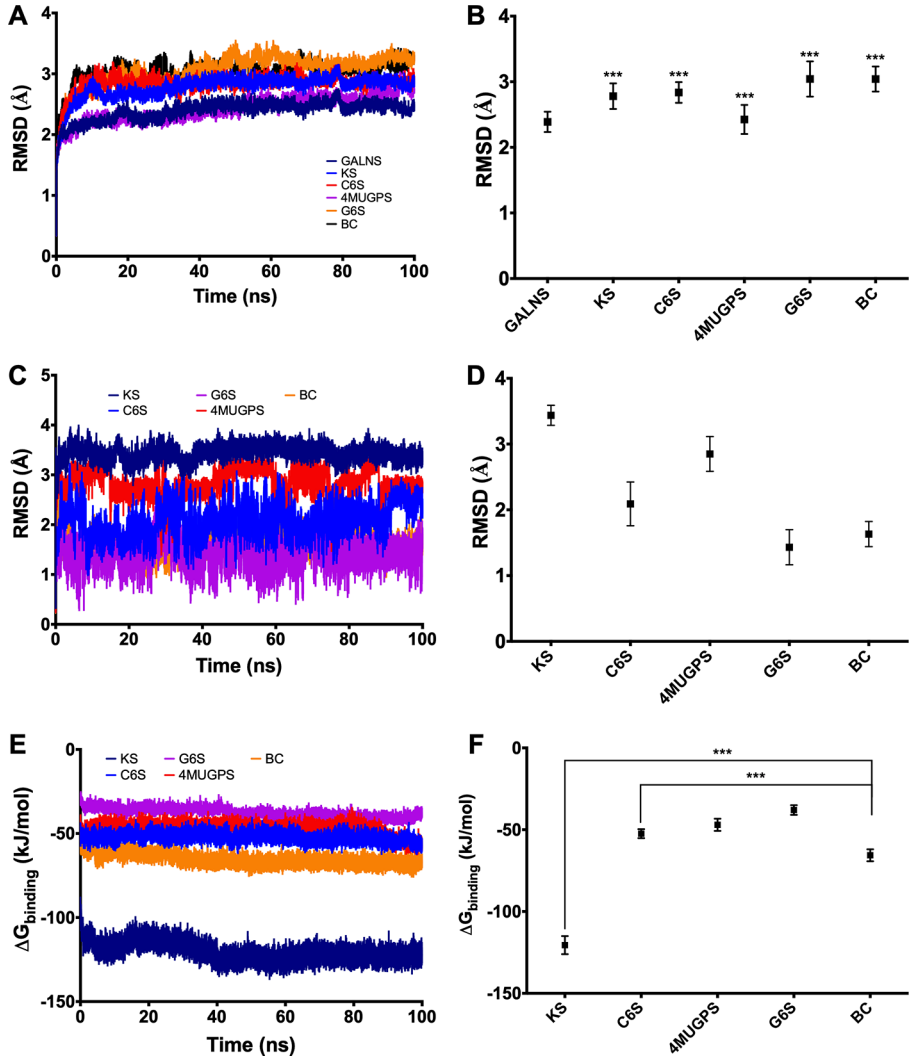

Figure 1. Molecular dynamics simulation for GALNS and ligands. Simulations were carried out for 100 ns using GROMAC 4.5.5. The trajectories were analyzed by RMSD for the protein docked with each ligand (A), for the ligands (C), and by the affinity energy (E). Average of RMSD for the protein docked with each ligand (B), the ligands (D), and the affinity energy (F) are also presented. KS: keratan sulfate, C6S: chondroitin-6-sulfate, G6S: galactose-6-sulfate, 4MUGPS: 4-methylumbelliferyl-β-D-galactopyranoside-6-sulfate, and BC: bromocriptine (ANOVA Holm-Šidák test *** $p < 0.0001$, $n = 50001$).

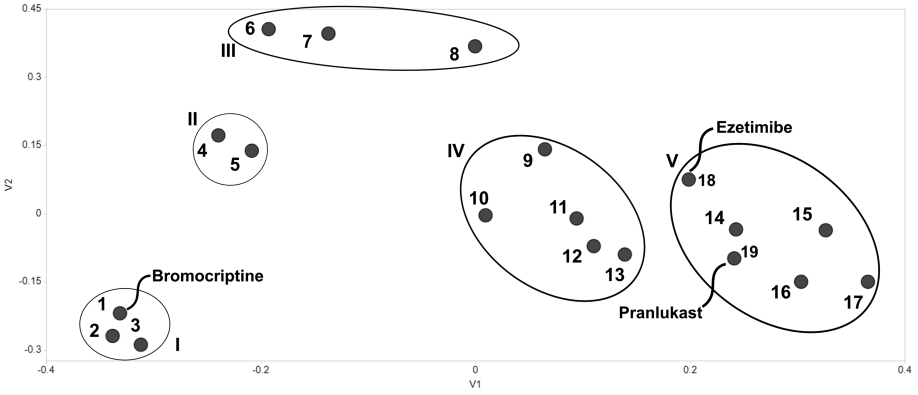

Figure 2. Clustering of top 20 hits interacting with human GALNS. (1) Bromocriptine, (2) Dihydroergotamine, (3) Ergocristine, (4) Algestone acetophenide, (5) Dexamethasone-21-sulfobenzoate, (6) Picrotin, (7) ZINC03872491, (8) Nimorazole, (9) Penfluridol, (10) Palosuran, (11) Bisoctrizole, (12) Plevitrexed, (13) (6S,12ar)-Tadalafil, (14) Lumacaftor, (15) Talniflumate, (16) Tarazepide, (17) Devazepide, (18) Ezetimibe, and (19) Pranlukast.

acetylgalactosamine-6-sulfate sulfatase (GALNS, EC 3.1.6.4).[1] GALNS deficiency leads to the lysosomal accumulation of the glycosaminoglycans keratan sulfate (KS) and chondroitin-6-sulfate (C6S).[1] Patients under enzyme replacement therapy

https://dx.doi.org/10.1021/acsmedchemlett.0c00042
ACS Med. Chem. Lett. 2020, 11, 1377−1385

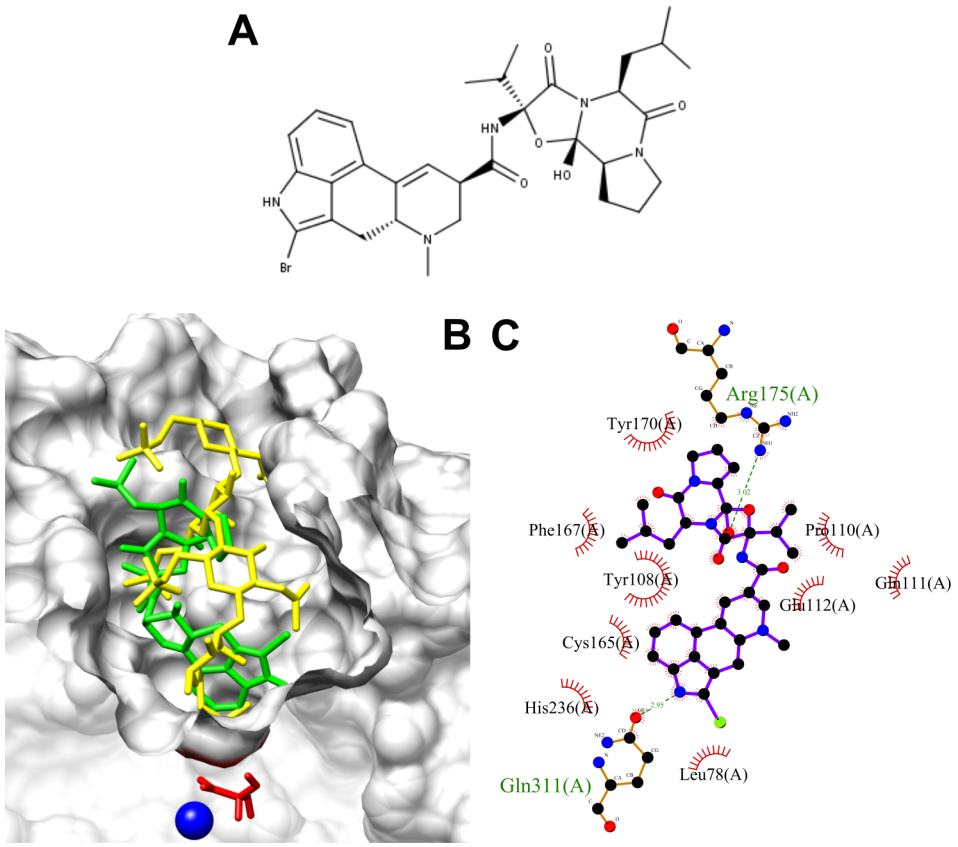

Figure 3. (A) BC structure. (B) *In silico* molecular docking keratan sulfate (yellow), and BC (green) within the active site cavity of human GALNS (PDB: 4FDI). Catalytic residue (FGly79) and calcium ion from GALNS are shown in red and blue, respectively. (C) Protein−ligand interactions between human GALNS and BC. Green and black residues are residues interacting through hydrogen bond and hydrophobic interactions, respectively.

(ERT) with elosulfase alfa have shown considerable improvements in clinical symptoms of the disease.[2] Unfortunately, ERT has limited effects correcting the skeletal, corneal, and cardiac abnormalities,[2] as well as abnormal growth.[3] On the other hand, although hematopoietic stem cell transplantation has shown some clinical benefits,[4] this is a high-risk procedure with many possible complications and high mortality. In this sense, it is necessary to improve the efficacy and safety of current therapies as well as to develop novel treatment alternatives. Gene therapy is under preclinical evaluation,[5] while alternative ERT delivery systems[6] and hosts for producing recombinant GALNS[7−9] and novel enzymes[10] have been proposed.

Genotype-phenotype correlations have predicted that GALNS mutations may affect the hydrophobic core, salt bridges, ligand affinity, solvent-accessible surface, and N-glycosylation sites.[11−14] It has been proposed then the use of small molecules, called pharmacological chaperones (PCs), to promote the correct folding of misfolded or unfolded proteins, as well as the proper intracellular trafficking of a mutated protein.[15] Compared to ERT, PCs have advantages such as a wide tissue distribution profile, reduced immunogenicity issues, and ease of administration via oral route.[16,17] In LSDs, PCs have been experimentally tested on Fabry disease (migalastat), Gaucher disease, Pompe disease, gangliosidosis (GM1 and GM2), MPS II, and MPS IVB.[18] Recently, we reported ezetimibe and pranlukast as the first PCs for MPS IVA.[19] These molecules increased the activity and thermostability of human recombinant GALNS (hrGALNS), reduced the lysosomal mass, and normalized the abnormal autophagic processes in MPS IVA patient-derived fibroblasts. In this work, we describe the identification and characterization of bromocriptine (BC) as a novel PC for MPS IVA based on a virtual screening strategy using the GALNS crystal structure (PDB 4FDI). Experimental procedures are detailed in Supporting Information (SI).

We started by making the computational validation of GALNS crystal structure and identified the presence of an isomeric variable residue (Val283). Geometrically, GALNS Val283 residue has angle changes inferior to 3° between the bonds for the isomeric variants and an orientation change of 180° between isoforms for methyl groups in the radical nonpolar aliphatic region (Figure S1A (SI)). The transition probability of this residue between isomeric states was 50%; then both isomeric variants are equally probable in GALNS structure. Nevertheless, the lowest RMSD was predicted for the protein backbone of State 1 ($p < 0.0001$) (Figure S1B (SI)). We thus performed all molecular dockings and virtual screening using State 1 of the protein, considering that a lower RMSD is associated with higher protein stability and, hereby, a better computational GALNS representation.

With this protein backbone selected and given that no substrate-binding analysis has been reported for this GALNS crystal structure,[13] we then modeled the interactions between natural and artificial GALNS substrates with this GALNS crystal structure. Table 1 summarizes the predicted interactions between GALNS crystal structure and ligands. Leu78, FGly79, Tyr108, His142, Asp, 233, His236, Ile294, Lys310,

https://dx.doi.org/10.1021/acsmedchemlett.0c00042
ACS Med. Chem. Lett. 2020, 11, 1377−1385

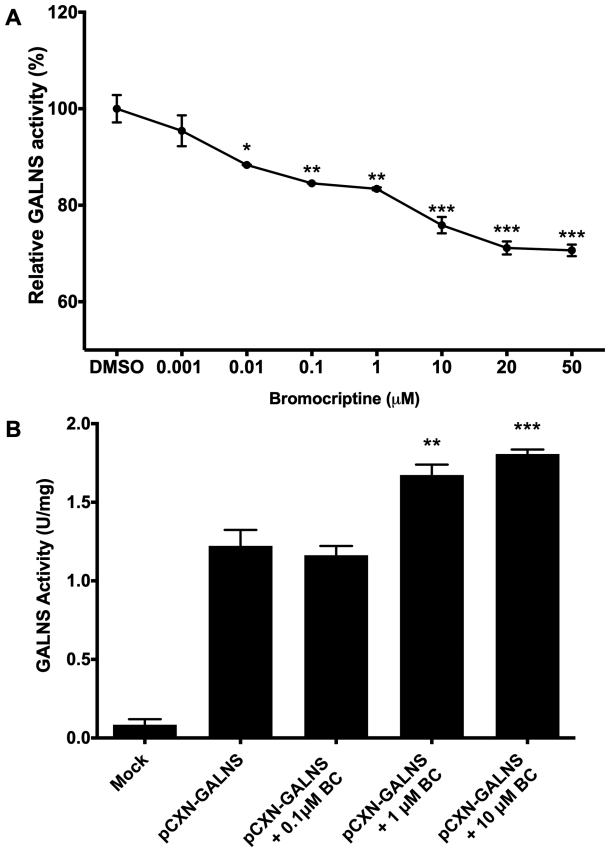

Figure 4. (A) Inhibitory assay for hrGALNS incubated with fluorogenic substrate 4MUGPS with or without BC. The results are reported as the percentage of the enzyme activity relative to the control group. (B) Effect of BC on the production of hrGALNS in HEK293 cells. Cells were transfected with plasmid pCXN-GALNS and treated with different concentrations of BC. (ANOVA Holm-Šidák test * $p < 0.01$, ** $p < 0.001$, *** $p < 0.0001$, $n = 3$.)

Trp520, and Ser521 were common residues interacting with selected substrates (Figure S2 (SI)). Asn106, Pro110, Glu112, Lys140, Phe167, Arg175, Gln311, Ile416, Phe418, Cys489, and His522 were also predicted as residues that interacted with the evaluated substrates (Figure S2 (SI)). Compared with our previous study, where a modeled GALNS structure was used and both KS and C6S were able to fit within the GALNS active cavity,[14] the use of GALNS crystal structure allowed us to predict more GALNS-C6S interactions than those predicted with the modeled structure. Among the interacting residues, Trp520, Ser521, and His522, which are located in the protein C-terminus, were predicted to interact with KS, C6S, and 4MUGPS. These interactions were not previously predicted using the modeled GALNS structure, which could be due to differences observed in the C-terminal domain between GALNS modeled and crystal structures.[14] This prediction correlates with the crystal structure analysis, which suggests that GALNS C-terminus could represent a barrier for accessing the active cavity, contributing to substrate selectivity of the enzyme.[13] Furthermore, a comparison of interacting residues in GALNS active site with that of paralogous sulfatases, such as iduronate-2-sulfatase and arylsulfatase C, suggests that residues FGly79, Lys140, His236, Lys310, and Gln311 are important for the enzyme−substrate interaction.[20,21]

Predicted affinity energy between GALNS and substrates suggests a lower affinity for the artificial substrate 4MUGPS (−5.4 kcal mol^{-1}) than for KS (−7.7 kcal mol^{-1}) and C6S (−6.3 kcal mol^{-1}) (Table 2). This prediction correlates well with the one obtained using the modeled GALNS structure[14] and with the affinity results reported for arylsulfatase A with natural and artificial substrates.[22] A key transformation in the catalytic site of sulfatases is the transformation of a cysteine precursor present in their active site to formylglycine (FGly).[21] We then modeled the effect of FGly79 presence in the active cavity on the affinity energy since previous studies using modeled GALNS structure have Cys instead of FGly.[14] FGly79 presence in the active site reduced the affinity energy for all evaluated substrates (Table 2), which implies a higher affinity. These results suggest a key role of FGly79 not only in GALNS activity[23] but also in the GALNS−substrate interaction. Due to the importance of FGly79 in GALNS biological activity and predicted role in GALNS−substrate interaction, further modeling was done using the crystal GALNS structure with FGly79 at the active cavity.

Molecular dynamics simulations predicted significantly higher RMSD values for GALNS docked with substrates (KS, C6S, 4MUGPS, and G6S) than for the free protein, suggesting that GALNS−substrate interactions may induce a structural change in GALNS. These values, however, were not significantly different among the evaluated substrates ($p > 0.05$) (Figures 1A−B). It was also predicted that all substrates were stable within the active cavity during the simulation time (Figures 1C−D). Modeled enzyme−substrate interaction showed that GALNS has the highest affinity for KS among the evaluated substrates (−120.5 ± 5.5 kJ mol^{-1}), followed by C6S (−52.4 ± 2.8 kJ mol^{-1}), 4MUGPS (−46.9 ± 3.7 kJ mol^{-1}), and G6S (−37.9 ± 2.9 kJ mol^{-1}) (Figures 1E−F). These results correlate well with previous simulations using an *in-silico* GALNS structure model[14] and the docking results presented above.

We then proceeded to identify potential PCs that bind to human GALNS via a virtual screening strategy against the ZINC In Man subset from ZINC,[19] similar to the one previously reported using the modeled GALNS structure where ezetimibe and pranlukast were assessed as potential PCs for GALNS.[14] In this study, we used the crystal structure of human GALNS with the FGly79 residue in the active cavity. A structure-based clustering of the top 20 hits after virtual screening (Table S1 (SI)) allowed the identification of five clusters, showing a wide variety of structures that can fit within the GALNS active cavity (Figure 2). Besides structural similarities observed among the evaluated compounds, some functional similarities were also observed within the members of some clusters. For instance, cluster I includes molecules that interact with dopamine and alpha-adrenergic receptors; while compounds in cluster II have a corticoid-like structure and share the mineralocorticoid receptor as a potential common target. Conversely, no common activity or target was identified for compounds in clusters III, IV, and V.

Our rationale for the selection of a potential PC for human GALNS lies on potential side effects of the molecule and its safety. These are factors of major concern in long-term drug administration, especially in a daily treatment scheme, which is usually required by MPS IVA patients. We did not consider for further investigation analgesic, antibiotic, antineoplastic, antiestrogen, antipsychotic, and vasodilator drugs listed in the top 20 hits, given their potential side effects during long-term administration (Table S1 (SI)). Among the top 20 hits, BC (Figure 3A) was ranked as the first among the 11,421

https://dx.doi.org/10.1021/acsmedchemlett.0c00042
ACS Med. Chem. Lett. 2020, 11, 1377−1385

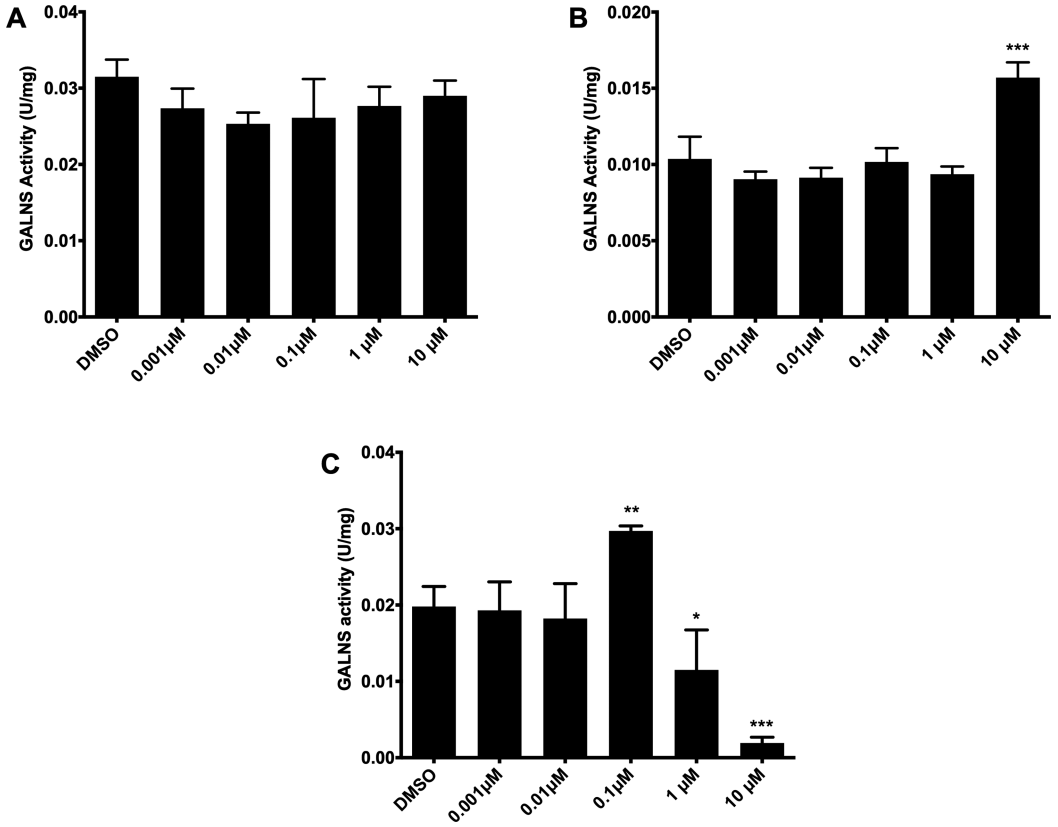

Figure 5. Effect of BC on GALNS activity in MPS IVA patient fibroblasts. GM00958 (A, p.A393S), GM00593 (B, p.R386C/p.F285del), and GM01361 (C, p.R61W/p.W405_T406del) MPS IVA fibroblasts were treated with different concentrations of bromocriptine for 48 h after which the GALNS activity was measured in the cell lysate. All assays were performed in triplicate (ANOVA Holm-Šidák test ** $p < 0.001$, *** $p < 0.0001$, $n = 3$).

compounds present in ZINC In Man subset. Moreover, two structural analogs of BC (ZINC71928211 and ZINC71928212) were also among the top 20. BC is a dopamine receptor agonist administered orally, with strong activity against D2 dopamine receptors and a partial activity against the D1 dopamine receptors in the central nervous system.[24] BC was first approved by the FDA in 1978, and current indications include the treatment of symptomatic Parkinson's disease and spastic and extrapyramidal disorders (10−40 mg per day), hyperprolactinemia and acromegaly (5−7.5 mg per day), and diabetes mellitus type II (0.8 mg per day).[24,25] Several repurposing studies of BC have shown the potential applications as an antitumoral,[26] antiviral (against Zika virus), and antiparasitic (against *Trypanosoma cruzi*) agent.[27,28] Moreover, BC has shown a good safety profile in children and adolescents,[29] which represent an important population among MPS IVA patients.[30] BC presents potential side effects that include nausea, vomiting, dizziness, and fatigue; while more serious and rare (<0.1%) side effects include fibrosis and cardiovascular incidents.[24] However, the incidence of most of these side effects is relatively low (<8%), except for dizziness that can be as high as 49%.[31] We thus select BC for further study as a GALNS PC, given it was ranked first in the virtual screening, has a wide therapeutic window and good safety profile, and has side effects that can be considered mild. BC does not share the same cluster of ezetimibe and pranlukast, previously reported as GALNS PCs,[19] suggesting that they do not share common properties (Figure 2), making BC an interesting GALNS PC candidate. Among the top 20 hits, other potential PCs were identified. For instance, tarazepide, talniflumate, devazipide, and lumacaftor were clustered with ezetimibe and pranlukast. These molecules share structural characteristics which is a starting point for the design of novel GALNS PCs.

Docking experiments were then carried out to evaluate the interaction between BC and human GALNS (Figure 3). BC docks into the GALNS active cavity in a similar pose to that predicted for KS (Figure 3B), with an affinity energy of −10.8 kcal mol^{-1}. BC was predicted to interact with the following GALNS residues: Leu78, Tyr108, Pro110, Gln111, Glu112, Cys165, Phe167, Tyr170, Arg175, His236, and Gln311, which are similar to those predicted for natural GALNS substrates (Figure 3C). Molecular dynamics simulations predicted that BC induces similar structural changes in GALNS than those observed for natural GALNS substrates (Figure 1B). BC showed an average binding energy of −65.6 ± 3.65 kJ mol^{-1}, which is significantly higher than that for KS (−120.5 ± 5.5 kJ/mol) (Figure 1F), suggesting that BC will not compete with GALNS natural substrate within the lysosome.

We then assessed the BC chaperone activity. We first used hrGALNS produced in *P. pastoris*,[8,32] which has been previously used in the characterization of PCs for MPS IVA.[19] We evaluated the interaction of BC with hrGALNS through an inhibition assay. An inhibition of up to 30% was observed between 0.001 and 50 μM of BC (Figure 4A), suggesting that BC binds to the active cavity of the enzyme and a direct binder of GALNS. This reduction in the enzyme activity is lower than the one observed with ezetimibe and

https://dx.doi.org/10.1021/acsmedchemlett.0c00042
ACS Med. Chem. Lett. 2020, 11, 1377−1385

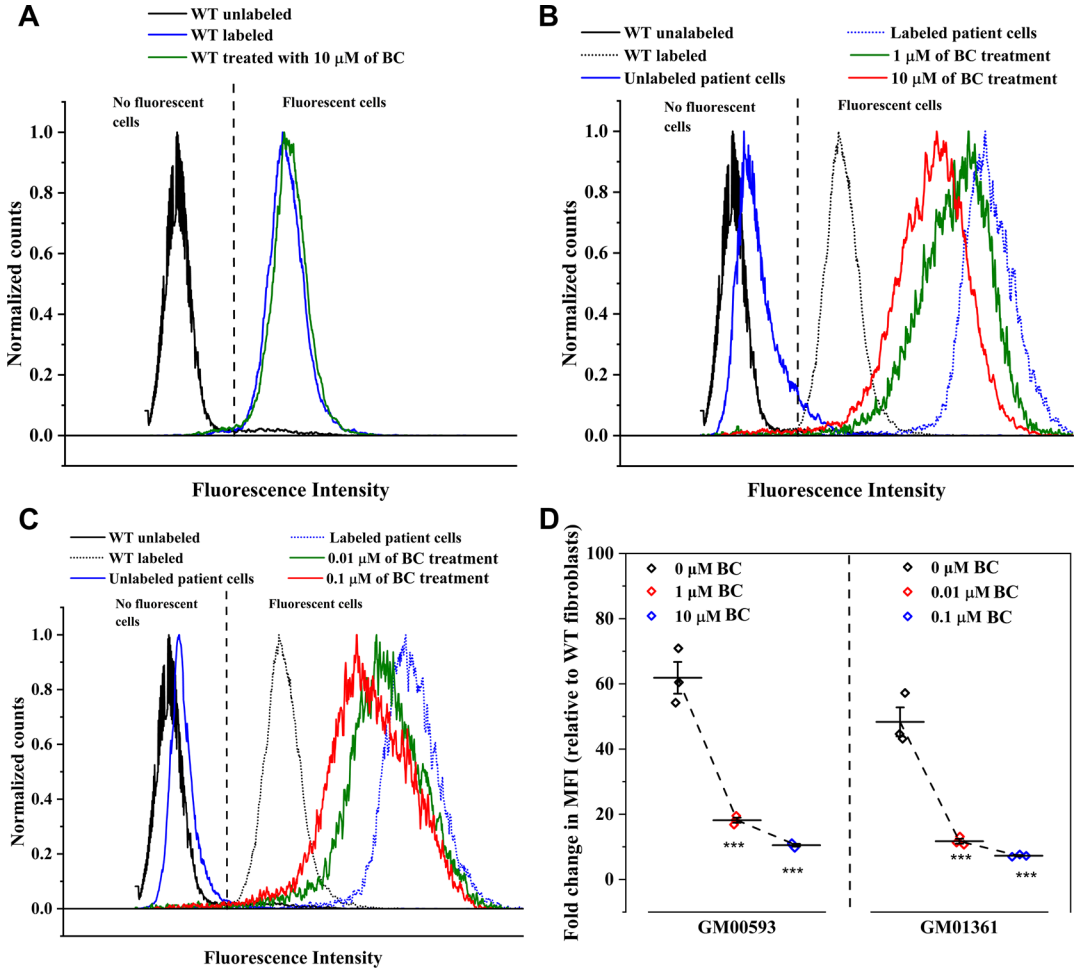

Figure 6. Normalized histogram overlays of wild type fibroblast (WT, A) and MPS IVA patient's fibroblast (GM00593, B, and GM01361, C) untreated and treated with BC. (D) Fold change in MFI relative to the control group, labeled WT fibroblast, was calculated. Three independent experiments per BC treatment and cell source were analyzed via flow cytometry (***, $p < 0.001$).

pranlukast, which was 40% and 50%, respectively, at a concentration of 10 μM[19]. However, we did not observe any correlation between enzyme inhibition and binding energy. For instance, ezetimibe and pranlukast showed enzyme activity inhibitions of 40 and 50%, with a predicted binding energy of −76.7 and −52.5 kJ/mol, respectively; while BC showed an activity reduction of up to 30% with a binding energy of −65.6 kJ/mol.

We then evaluated the effect of adding BC during hrGALNS production in HEK293 cells. Compared to DMSO treated cells, BC treatment showed a significant ($p < 0.001$) increase in GALNS activity. It was observed activities 1.36- and 1.48-fold higher than the control at BC concentrations of 1 and 10 μM, respectively (Figure 4B). Although this increment in GALNS activity is similar to that observed with ezetimibe and pranlukast, it is important to note that they were obtained at significantly higher BC concentration (1 and 10 μM) than the one used for ezetimibe and pranlukast (0.001 μM).[19] Despite the fact that BC needs higher concentrations to those observed for ezetimibe and pranlukast to improve GALNS activity, these results show the potential application of BC as a PC to increase the activity of a hrGALNS.

To further challenge the potential PC activity of BC, we assessed its effect on MPS IVA fibroblasts GM00593 (p.R386C/p.F285del), GM00958 (p.A393S), and GM01361 (p.R61W/p.W405_T406del).[19] In the case of MPS IVA fibroblasts GM00958 (p.A393S), the treatment with BC did not induce any increment in GALNS activity (Figure 5A). These results suggest that this mutation is not responsive to BC treatment and differs from those results obtained with ezetimibe and pranlukast, for which a significant increment in GALNS activity (up to 2.5-fold) was observed.[19] On the other hand, GM00593 (p.R386C/p.F285del) fibroblasts showed a 1.52-fold increase in GALNS activity at 10 μM, while GM01361 (p.R61W/p.W405_T406del) fibroblasts presented a 1.50-fold increase at 0.1 μM (Figures 5B−C). The observed enhancement in GALNS activity for GM00593 fibroblasts is lower than the one obtained with ezetimibe (2.5-fold increase with 0.01 μM), while no increase in enzyme activity was previously observed with pranlukast. The enhancement in the activity of GALNS induced by BC using GM01361 fibroblasts is similar to that previously observed with ezetimibe (1.6-fold) and pranlukast (1.5-fold),[19] suggesting that mutations present in these fibroblasts are easy to treat by PC therapy since they respond to different PCs. However, GALNS activity was significantly reduced in these fibroblasts at 1 and 10 μM BC (Figure 5C). As has been reported, PCs are mainly competitive inhibitors that bind to the enzyme active cavity in a mutation-dependent manner.[16,17] In this sense, the reduction of enzyme activity in GM01361 fibroblasts may suggest that these

https://dx.doi.org/10.1021/acsmedchemlett.0c00042
ACS Med. Chem. Lett. 2020, 11, 1377−1385

mutations are more sensitive to BC than those present in GM00593 fibroblasts. Overall, these results show the PC activity of BC over mutated GALNS with a marked mutation-dependent chaperone activity, suggesting that its use should be on an individualized patient basis.

Although the BC concentrations used in this study agree with those used in previous *in vitro* studies of BC (i.e., ∼0.6 to 100 μM),[27,33−36] the BC pharmacokinetics evaluation in Parkinson's disease patients has shown that total plasma concentrations are between ∼0.01 μM (6.5 μg L^{-1}) and 0.25 μM (165 μg L^{-1}), with a 90 to 96% protein binding, suggesting a very low concentration of the free drug.[37] In this sense, the BC concentrations described in the present study are significantly higher than those found in human plasma, which limits the direct translation of this drug to the clinics. However, BC can be used as a starting point for the *de novo* development of molecules with a chaperone activity in MPS IVA.

Previously, we showed that measurement of lysosomal mass by LysoTracker staining can be used as a phenotypic assay for drug screening in MPS IVA patient-derived cells.[19] Subsequently, wild-type and MPS IVA patient fibroblasts GM00593 and GM01361 were exposed to different BC concentrations, labeled with Lysotracker deep red, and analyzed via flow cytometry. Wild-type cell population treated with BC were not affected (Figure 6A), suggesting that BC does not have any positive or deleterious effect on wild-type GALNS. In fact, we did not observe any change in GALNS activity on BC treated wild-type fibroblasts compared to untreated fibroblasts (data not shown). On the other hand, the histogram of MPS IVA patient fibroblasts treated BC exhibits a leftward shifting with respect to the untreated group histogram (Figure 6B−C), suggesting a lysosomal mass reduction. To quantify this change, we assessed the fold change in the median fluorescence intensity (MFI) relative to the control, i.e. wild-type fibroblasts at the same experimental condition (Figure 6D). GM00593 fibroblast treated with 1 and 10 μM of BC showed a relative fold change in MFI from 61.8 ± 8.4 to 18.2 ± 1.3 and 10.5 ± 0.7, respectively. Similarly, GM01361 fibroblast showed a reduction from 48.3 ± 7.7 to 11.7 ± 1.3 and 7.3 ± 0.3 after being treated with 0.01 and 0.1 μM of BC, respectively (Figure 6D). Compared to the enzyme activity test, it was unexpected the observed reduction in the fold change in MFI for GM00593 and GM01361 fibroblasts after treatment with 1 and 0.01 μM BC, respectively. This discrepancy in the observed trends could be explained by differences between techniques and their sensitivity. Nevertheless, these results showed that BC not only increases GALNS activity but also can induce a reduction of lysosomal mass.

In conclusion, we identified and characterized BC as a novel PC for GALNS, which binds to hrGALNS and increases the activity of the enzyme during its production in mammalian cells (HEK293 cells). It is noteworthy that this compound also increased GALNS activity in MPS IVA fibroblasts, in a mutation-dependent manner. Nevertheless, higher concentrations of BC were needed compared to those previously reported for ezetimibe and pranlukast. These results confirm that our strategy allows the identification of PC for GALNS and confirm ezetimibe as the best PC described for this enzyme. Nevertheless, medicinal chemistry optimization could improve the chaperone activity of BC. In addition, these results offer valuable information for the rational design of novel PC for GALNS. Overall, these results contribute to the consolidation of PCs as a potential therapy for MPS IVA and suggest that a similar strategy could be applied to the identification of PCs for other LSDs.

■ ASSOCIATED CONTENT

Supporting Information

The Supporting Information is available free of charge at https://pubs.acs.org/doi/10.1021/acsmedchemlett.0c00042.

Details of experimental procedures, top 20 hits of the compounds interacting with GALNS after the virtual screening, geometrical isomers of Val283 in the GALNS protein structure, and protein−substrates interactions between human GALNS and the natural artificial substrates (PDF)

■ AUTHOR INFORMATION

Corresponding Author

Carlos J. Alméciga-Díaz − *Institute for the Study of Inborn Errors of Metabolism, Faculty of Science, Pontificia Universidad Javeriana, Bogotá, D.C. 110231, Colombia;* orcid.org/0000-0001-6484-1173; Phone: +57-1 3208320; Email: cjalmeciga@javeriana.edu.co; Fax: +57-1 3208320

Authors

Sergio Olarte-Avellaneda − *Institute for the Study of Inborn Errors of Metabolism, Faculty of Science, Pontificia Universidad Javeriana, Bogotá, D.C. 110231, Colombia; Pharmacy Department, Faculty of Science, Universidad Nacional de Colombia, Bogotá, D.C. 11001, Colombia*

Jacobo Cepeda Del Castillo − *Institute for the Study of Inborn Errors of Metabolism, Faculty of Science, Pontificia Universidad Javeriana, Bogotá, D.C. 110231, Colombia*

Andrés Felipe Rojas-Rodriguez − *Computational and Structural Biochemistry, Biochemistry and Nutrition Department, Faculty of Science, Pontificia Universidad Javeriana, Bogotá, D.C. 110231, Colombia*

Oscar Sánchez − *Neurobiochemistry and Systems Physiology, Biochemistry and Nutrition Department, Faculty of Science, Pontificia Universidad Javeriana, Bogotá, D.C. 110231, Colombia*

Alexander Rodríguez-López − *Institute for the Study of Inborn Errors of Metabolism, Faculty of Science and Chemistry Department, Faculty of Science, Pontificia Universidad Javeriana, Bogotá, D.C. 110231, Colombia*

Diego A. Suárez García − *Institute for the Study of Inborn Errors of Metabolism, Faculty of Science, Pontificia Universidad Javeriana, Bogotá, D.C. 110231, Colombia; Faculty of Medicine, Universidad Nacional de Colombia, Bogotá, D.C 11001, Colombia;* orcid.org/0000-0001-9519-4706

Luz Mary Salazar Pulido − *Chemistry Department, Faculty of Science, Universidad Nacional de Colombia, Bogotá, D.C. 11001, Colombia*

Complete contact information is available at: https://pubs.acs.org/10.1021/acsmedchemlett.0c00042

Author Contributions

S.O.-A. performed the bioinformatics analysis and simulations and wrote and revised the manuscript. J.C.D.C. performed the in vitro experiments and revised the manuscript. A.F.R.-R. performed the bioinformatics analysis and simulations and wrote and revised the manuscript. O.F.S. conceived and

https://dx.doi.org/10.1021/acsmedchemlett.0c00042
ACS Med. Chem. Lett. 2020, 11, 1377−1385

designed the experiments and wrote and revised the manuscript. A.R.-L. conceived and designed the experiments and revised the manuscript. D.A.S. performed in vitro experiments and revised the manuscript. L.M.S.P. conceived and designed bioinformatics analysis and revised the manuscript. C.J.A.-D. conceived and designed the bioinformatics analysis and *in vitro* experiments and wrote and revised the manuscript.

Notes

The authors declare no competing financial interest.

■ ACKNOWLEDGMENTS

CJAD was supported by Pontificia Universidad Javeriana [PPTA #7520] and the Ministry of Science, Technology and Innovation, Colombia [Grant ID 5174 - contract No. 120356933205, and Grant ID 5170 - contract No. 120356933427]. DAS and OFS received a young researcher fellowship (Contract 829-2018 − PPTA # 8728) and a postdoctoral fellowship (Grant ID 811-2018), respectively, from the Ministry of Science, Technology and Innovation, Colombia. The content of the article has not been influenced by the sponsors.

■ ABBREVIATIONS LIST:

MPS, mucopolysaccharidosis; MPS IVA, mucopolysaccharidosis type IVA; LSD, lysosomal storage disease; GALNS, *N*-acetylgalactosamine-6-sulfate sulfatase; KS, keratan sulfate; C6S, chondroitin-6-sulfate; PC, pharmacological chaperone; BC, bromocriptine; ERT, enzyme replacement therapy; hrGALNS, human recombinant GALNS; FGly, formilglycine; RMSD, root mean squared distance; G6S, galactose-6-sulfate; 4MUGPS, 4-methylumbelliferyl-β-D-galactopyranoside-6-sulfate.

■ REFERENCES

(1) Sawamoto, K.; Alméciga-Díaz, C. J.; Mason, R. W.; Orii, T.; Tomatsu, S. Mucopolysaccharidosis type IVA: clinical features, biochemistry, diagnosis, genetics, and treatment. In *Mucopolysaccharidoses update (2 volume set)*; Tomatsu, S., Lavery, C., Giugliani, R., Harmatz, P., Scarpa, M., Węgrzyn, G., Orii, T., Eds.; Nova Science Publishers, Inc.: Hauppauge, NY, 2018; Vol. *I*, pp 235−272.

(2) Tomatsu, S.; Sawamoto, K.; Shimada, T.; Bober, M. B.; Kubaski, F.; Yasuda, E.; Mason, R. W.; Khan, S.; Alméciga-Díaz, C. J.; Barrera, L. A.; Mackenzie, W. G.; Orii, T. Enzyme replacement therapy for treating mucopolysaccharidosis type IVA (Morquio A syndrome): effect and limitations. *Expert Opin. Orphan Drugs* **2015**, *3* (11), 1279−1290.

(3) Doherty, C.; Stapleton, M.; Piechnik, M.; Mason, R. W.; Mackenzie, W. G.; Yamaguchi, S.; Kobayashi, H.; Suzuki, Y.; Tomatsu, S. Effect of enzyme replacement therapy on the growth of patients with Morquio A. *J. Hum. Genet.* **2019**, *64*, 625−635.

(4) Yabe, H.; Tanaka, A.; Chinen, Y.; Kato, S.; Sawamoto, K.; Yasuda, E.; Shintaku, H.; Suzuki, Y.; Orii, T.; Tomatsu, S. Hematopoietic stem cell transplantation for Morquio A syndrome. *Mol. Genet. Metab.* **2016**, *117* (2), 84−94.

(5) Alméciga Díaz, C.; Montaño, A.; Barrera, L.; Tomatsu, S. Tailoring the AAV2 capsid vector for bone-targeting. *Pediatr. Res.* **2018**, *84* (4), 545−551.

(6) Álvarez, J. V.; Herrero Filgueira, C.; González, A. F.; Colón Mejeras, C.; Beiras Iglesias, A.; Tomatsu, S.; Blanco Méndez, J.; Luzardo Álvarez, A.; Couce, M. L.; Otero Espinar, F. J. Enzyme-Loaded gel core nanostructured lipid carriers to improve treatment of lysosomal storage diseases: formulation and in vitro cellular studies of elosulfase alfa-loaded systems. *Pharmaceutics* **2019**, *11* (10), 522

(7) Mosquera, A.; Rodríguez, A.; Soto, C.; Leonardi, F.; Espejo, A.; Sánchez, O. F.; Alméciga-Díaz, C. J.; Barrera, L. A. Characterization of a recombinant N-acetylgalactosamine-6-sulfate sulfatase produced in E. coli for enzyme replacement therapy of Morquio A disease. *Process Biochem.* **2012**, *47*, 2097−2102.

(8) Rodriguez-Lopez, A.; Pimentel-Vera, L. N.; Espejo-Mojica, A. J.; Van, H. A.; Tiels, P.; Tomatsu, S.; Callewaert, N.; Almeciga-Diaz, C. J. Characterization of human recombinant N-acetylgalactosamine-6-sulfate sulfatase produced in Pichia pastoris as potential enzyme for mucopolysaccharidosis IVA treatment. *J. Pharm. Sci.* **2019**, *108* (8), 2534−2541.

(9) Rodriguez, A.; Espejo, A. J.; Hernandez, A.; Velasquez, O. L.; Lizaraso, L. M.; Cordoba, H. A.; Sanchez, O. F.; Almeciga-Diaz, C. J.; Barrera, L. A. Enzyme replacement therapy for Morquio A: an active recombinant N-acetylgalactosamine-6-sulfate sulfatase produced in Escherichia coli BL21. *J. Ind. Microbiol. Biotechnol.* **2010**, *37* (11), 1193−1201.

(10) Sawamoto, K.; Tomatsu, S. Development of substrate degradation enzyme therapy for Mucopolysaccharidosis IVA murine model. *Int. J. Mol. Sci.* **2019**, *20* (17), 4139

(11) Tomatsu, S.; Montaño, A.; Nishioka, T.; Gutierrez, M.; Peña, O.; Trandafirescu, G.; Lopez, P.; Yamaguchi, S.; Noguchi, A.; Orri, T. Mutation and polymorphism spectrum of the GALNS gene in mucopolysaccharidosis IVA (Morquio A). *Hum. Mutat.* **2005**, *26*, 500−512.

(12) Sukegawa, K.; Nakamura, H.; Kato, Z.; Tomatsu, S.; Montaño, A. M.; Fukao, T.; Toietta, G.; Tortora, P.; Orii, T.; Kondo, N. Biochemical and structural analysis of missense mutations in N-acetylgalactosamine-6-sulfate sulfatase causing mucopolysaccharidosis IVA phenotypes. *Hum. Mol. Genet.* **2000**, *9* (9), 1283−1290.

(13) Rivera-Colon, Y.; Schutsky, E. K.; Kita, A. Z.; Garman, S. C. The structure of human GALNS reveals the molecular basis for mucopolysaccharidosis IV A. *J. Mol. Biol.* **2012**, *423* (5), 736−751.

(14) Olarte-Avellaneda, S.; Rodríguez-López, A.; Alméciga-Díaz, C. J.; Barrera, L. A. Computational analysis of human N-acetylgalactosamine-6-sulfate sulfatase enzyme: an update in genotype-phenotype correlation for Morquio A. *Mol. Biol. Rep.* **2014**, *41* (11), 7073−7088.

(15) Arakawa, T.; Ejima, D.; Kita, Y.; Tsumoto, K. Small molecule pharmacological chaperones: from thermodynamic stabilization to pharmaceutical drugs. *Biochim. Biophys. Acta, Proteins Proteomics* **2006**, *1764* (11), 1677−1687.

(16) Valenzano, K. J.; Khanna, R.; Powe, A. C.; Boyd, R.; Lee, G.; Flanagan, J. J.; Benjamin, E. R. Identification and characterization of pharmacological chaperones to correct enzyme deficiencies in lysosomal storage disorders. *Assay Drug Dev. Technol.* **2011**, *9* (3), 213−235.

(17) Pereira, D. M.; Valentao, P.; Andrade, P. B. Tuning protein folding in lysosomal storage diseases: the chemistry behind pharmacological chaperones. *Chem. Sci.* **2018**, *9* (7), 1740−1752.

(18) Losada Díaz, J. C.; Cepeda del Castillo, J.; Rodriguez-López, E. A.; Alméciga-Díaz, C. J. Advances in the development of pharmacological chaperones for the mucopolysaccharidoses. *Int. J. Mol. Sci.* **2020**, *21* (1), 232.

(19) Almeciga-Diaz, C. J.; Hidalgo, O. A.; Olarte-Avellaneda, S.; Rodriguez-Lopez, A.; Guzman, E.; Garzon, R.; Pimentel-Vera, L. N.; Puentes-Tellez, M. A.; Rojas-Rodriguez, A. F.; Gorshkov, K.; Li, R.; Zheng, W. Identification of ezetimibe and pranlukast as pharmacological chaperones for the treatment of the rare disease mucopolysaccharidosis type IVA. *J. Med. Chem.* **2019**, *62* (13), 6175−6189.

(20) Demydchuk, M.; Hill, C. H.; Zhou, A.; Bunkóczi, G.; Stein, P. E.; Marchesan, D.; Deane, J. E.; Read, R. J. Insights into Hunter syndrome from the structure of iduronate-2-sulfatase. *Nat. Commun.* **2017**, *8*, 15786.

(21) Ghosh, D. Human sulfatases: a structural perspective to catalysis. *Cell. Mol. Life Sci.* **2007**, *64* (15), 2013−2022.

(22) Schenk, M.; Koppisetty, C. A.; Santos, D. C.; Carmona, E.; Bhatia, S.; Nyholm, P. G.; Tanphaichitr, N. Interaction of arylsulfatase-A (ASA) with its natural sulfoglycolipid substrates: a computational and site-directed mutagenesis study. *Glycoconjugate J.* **2009**, *26* (8), 1029−1045.

https://dx.doi.org/10.1021/acsmedchemlett.0c00042
ACS Med. Chem. Lett. 2020, 11, 1377−1385

(23) Hanson, S. R.; Best, M. D.; Wong, C. H. Sulfatases: structure, mechanism, biological activity, inhibition, and synthetic utility. *Angew. Chem., Int. Ed.* **2004**, *43* (43), 5736−5763.
(24) Michael, B. G.; Pfeiffer, R. F.; Thorner, M. O. Anniversary review: 50 years since the discovery of bromocriptine. *Eur. J. Endocrinol.* **2018**, *179* (2), R69−R75.
(25) Ozery, M.; Wadhwa, R. Bromocriptine. In *StatPearls*; StatPearls Publishing LLC: Treasure Island (FL), 2020. https://www.ncbi.nlm.nih.gov/pubmed/32310408.
(26) Yang, Y.; Mamouni, K.; Li, X.; Chen, Y.; Kavuri, S.; Du, Y.; Fu, H.; Kucuk, O.; Wu, D. Repositioning dopamine D2 receptor agonist bromocriptine to enhance docetaxel chemotherapy and treat bone metastatic prostate cancer. *Mol. Cancer Ther.* **2018**, *17* (9), 1859−1870.
(27) Chan, J. F.; Chik, K. K.; Yuan, S.; Yip, C. C.; Zhu, Z.; Tee, K. M.; Tsang, J. O.; Chan, C. C.; Poon, V. K.; Lu, G.; Zhang, A. J.; Lai, K. K.; Chan, K. H.; Kao, R. Y.; Yuen, K. Y. Novel antiviral activity and mechanism of bromocriptine as a Zika virus NS2B-NS3 protease inhibitor. *Antiviral Res.* **2017**, *141*, 29−37.
(28) Bellera, C. L.; Balcazar, D. E.; Alberca, L.; Labriola, C. A.; Talevi, A.; Carrillo, C. Application of computer-aided drug repurposing in the search of new Cruzipain inhibitors: discovery of amiodarone and bromocriptine inhibitory effects. *J. Chem. Inf. Model.* **2013**, *53* (9), 2402−2408.
(29) Catli, G.; Abaci, A.; Altincik, A.; Demir, K.; Can, S.; Buyukgebiz, A.; Bober, E. Hyperprolactinemia in children: clinical features and long-term results. *J. Pediatr. Endocrinol. Metab.* **2012**, *25* (11−12), 1123−1128.
(30) Montaño, A. M.; Tomatsu, S.; Gottesman, G.; Smith, M.; Orii, T. International Morquio A registry: clinical manifestation and natural course of Morquio A disease. *J. Inherited Metab. Dis.* **2007**, *30* (2), 165−174.
(31) Kuhn, M.; Letunic, I.; Jensen, L. J.; Bork, P. The SIDER database of drugs and side effects. *Nucleic Acids Res.* **2016**, *44* (D1), D1075−D1079.
(32) Rodríguez-López, A.; Alméciga-Díaz, C. J.; Sánchez, J.; Moreno, J.; Beltran, L.; Díaz, D.; Pardo, A.; Ramírez, A. M.; Espejo-Mojica, A. J.; Pimentel, L.; Barrera, L. A. Recombinant human N-acetylgalactosamine-6-sulfate sulfatase (GALNS) produced in the methylotrophic yeast Pichia pastoris. *Sci. Rep.* **2016**, *6*, 29329−29342.
(33) Morikawa, K.; Oseko, F.; Morikawa, S. Immunosuppressive activity of bromocriptine on human T lymphocyte function in vitro. *Clin. Exp. Immunol.* **1994**, *95* (3), 514−518.
(34) Kato, F.; Ishida, Y.; Oishi, S.; Fujii, N.; Watanabe, S.; Vasudevan, S. G.; Tajima, S.; Takasaki, T.; Suzuki, Y.; Ichiyama, K.; Yamamoto, N.; Yoshii, K.; Takashima, I.; Kobayashi, T.; Miura, T.; Igarashi, T.; Hishiki, T. Novel antiviral activity of bromocriptine against dengue virus replication. *Antiviral Res.* **2016**, *131*, 141−147.
(35) Jian, M.; Du, Q.; Zhu, D.; Mao, Z.; Wang, X.; Feng, Y.; Xiao, Z.; Wang, H.; Zhu, Y. Tumor suppressor miR-145−5p sensitizes prolactinoma to bromocriptine by downregulating TPT1. *J. Endocrinol. Investig.* **2019**, *42* (6), 639−652.
(36) Lara-Castillo, M. C.; Cornet-Masana, J. M.; Etxabe, A.; Banús-Mulet, A.; Torrente, M. Á.; Nomdedeu, M.; Díaz-Beyá, M.; Esteve, J.; Risueño, R. M. Repositioning of bromocriptine for treatment of acute myeloid leukemia. *J. Transl. Med.* **2016**, *14* (1), 261.
(37) Deleu, D.; Northway, M. G.; Hanssens, Y. Clinical pharmacokinetic and pharmacodynamic properties of drugs used in the treatment of Parkinson's disease. *Clin. Pharmacokinet.* **2002**, *41* (4), 261−309.

https://dx.doi.org/10.1021/acsmedchemlett.0c00042
ACS Med. Chem. Lett. 2020, 11, 1377−1385